PROCEEDINGS A

royalsocietypublishing.org/journal/rspa

Research

Cite this article: Idiart MI, Lahellec N, Suquet P. 2020 Model reduction by mean-field homogenization in viscoelastic composites. II. Application to rigidly reinforced solids. *Proc. R. Soc. A* **476**: 20200408.
http://dx.doi.org/10.1098/rspa.2020.0408

Received: 24 May 2020
Accepted: 28 September 2020

Subject Areas:
mathematical modelling, mechanics, thermodynamics

Keywords:
viscoelasticity, composites, homogenization, variational methods

Author for correspondence:
Martín I. Idiart
e-mail: martin.idiart@ing.unlp.edu.ar

Model reduction by mean-field homogenization in viscoelastic composites. II. Application to rigidly reinforced solids

Martín I. Idiart[1,2], Noel Lahellec[3] and Pierre Suquet[3]

[1]Centro Tecnológico Aeroespacial/Departamento de Aeronáutica, Facultad de Ingeniería, Universidad Nacional de La Plata, Avda. 1 esq. 47, La Plata B1900TAG, Argentina
[2]Consejo Nacional de Investigaciones Científicas y Técnicas (CONICET), CCT La Plata, Calle 8 No 1467, La Plata B1904CMC, Argentina
[3]Aix Marseille Univ, CNRS, Centrale Marseille, LMA UMR 7031, Marseille, France

MII, 0000-0003-3450-5560; PS, 0000-0001-9870-4919

The mean-field homogenization scheme proposed by Lahellec & Suquet (2007 *Int. J. Solids Struct.* **44**, 507–529 (doi:10.1016/j.ijsolstr.2006.04.038)) and revisited in a companion paper (Idiart *et al.* 2020 *Proc. R. Soc. A* 20200407 (doi:10.1098/rspa.2020.0407)) is applied to random mixtures of a viscoelastic solid phase and a rigid phase. Two classes of mixtures with different microstructural arrangements are considered. In the first class the rigid phase is dispersed within the continuous viscoelastic phase in such a way that the elastic moduli of the mixture are given exactly by the Hashin–Shtrikman formalism. In the second class, both phases are intertwined in such a way that the elastic moduli of the mixture are given exactly by the Self-Consistent formalism. Results are reported for specimens subject to various complex deformation programmes. The scheme is found to improve on earlier approximations of common use and even recover exact results under several circumstances. However, it can also generate highly inaccurate predictions as a result of the loss of convexity of the free-energy density. An auspicious procedure to partially circumvent this issue is advanced.

1. Introduction

The mean-field homogenization scheme proposed by Lahellec & Suquet [1] and revisited in a companion

THE ROYAL SOCIETY PUBLISHING

paper [2] is applied to random mixtures of a viscoelastic phase and a rigid phase serving as reinforcement. Two classes of mixtures with different microstructural arrangements are considered. In the first class the rigid phase is dispersed within the continuous viscoelastic phase in such a way that the microstructure is of the 'particulate' type. In the second class, both phases are intertwined in such a way that the microstructure is of the 'granular' type. The main purpose of the study is to assess the capabilities and limitations of the homogenization scheme to generate accurate estimates for complex viscoelastic systems. For conciseness, we begin by recalling the overall structure of the constitutive framework employed. For further details, the reader is referred to the companion paper and references therein.

We consider a representative volume element of a composite material made up of two constituent phases, and denote by Ω and $\Omega^{(r)}$ $(r=1,2)$ the domains occupied by the element and the phases within it, respectively, so that $\Omega=\Omega^{(1)}\cup\Omega^{(2)}$. Also, we denote by $\chi^{(r)}(\mathbf{x})$ and $c^{(r)}$ the characteristic function and volume fraction of each subdomain $\Omega^{(r)}$, respectively. In turn, volume averages over the entire element and over each subdomain are indicated as $\langle\cdot\rangle$ and $\langle\cdot\rangle^{(r)}$. We restrict attention to material systems with statistically isotropic microstructures.

The local viscoelastic response is described within the framework of generalized standard materials by constitutive relations of the form

$$\boldsymbol{\sigma}=\frac{\partial w}{\partial\boldsymbol{\varepsilon}}(\mathbf{x},\boldsymbol{\varepsilon},\boldsymbol{\alpha})\quad\text{and}\quad\frac{\partial w}{\partial\boldsymbol{\alpha}}(\mathbf{x},\boldsymbol{\varepsilon},\boldsymbol{\alpha})+\frac{\partial\varphi}{\partial\dot{\boldsymbol{\alpha}}}(\mathbf{x},\dot{\boldsymbol{\alpha}})=\mathbf{0}, \tag{1.1}$$

where $\boldsymbol{\varepsilon}$ and $\boldsymbol{\alpha}$ denote the infinitesimal and inelastic strains relative to a stress-free reference configuration, $\boldsymbol{\sigma}$ denotes the Cauchy stress, the dot over a variable denotes a time derivative, and the potential functions w and φ are, respectively, the Helmholtz free-energy density and the dissipation potential of the heterogeneous system, which can be expressed in terms of the corresponding phase potentials as

$$w(\mathbf{x},\boldsymbol{\varepsilon},\boldsymbol{\alpha})=\sum_{r=1}^{2}\chi^{(r)}(\mathbf{x})w^{(r)}(\boldsymbol{\varepsilon},\boldsymbol{\alpha})\quad\text{and}\quad\varphi(\mathbf{x},\dot{\boldsymbol{\alpha}})=\sum_{r=1}^{2}\chi^{(r)}(\mathbf{x})\varphi^{(r)}(\dot{\boldsymbol{\alpha}}). \tag{1.2}$$

Henceforth we identify with $r=1$ the viscoelastic solid phase and with $r=2$ the rigid phase and we assume that the rheology of the viscoelastic phase is isotropic and Maxwellian. The local potentials of the viscoelastic phase are thus given by

$$w^{(1)}(\boldsymbol{\varepsilon},\boldsymbol{\alpha})=\tfrac{1}{2}(\boldsymbol{\varepsilon}-\boldsymbol{\alpha})\cdot\mathbb{L}(\boldsymbol{\varepsilon}-\boldsymbol{\alpha})+\tfrac{1}{2}\boldsymbol{\alpha}\cdot\mathbb{H}\boldsymbol{\alpha}\quad\text{and}\quad\varphi^{(1)}(\dot{\boldsymbol{\alpha}})=\tfrac{1}{2}\dot{\boldsymbol{\alpha}}\cdot\mathbb{M}\dot{\boldsymbol{\alpha}} \tag{1.3}$$

with

$$\mathbb{L}=3\kappa\,\mathbb{J}+2\mu\,\mathbb{K},\quad\mathbb{H}=+\infty\,\mathbb{J}\quad\text{and}\quad\mathbb{M}=2\eta\,\mathbb{K}, \tag{1.4}$$

where $\mathbb{J}$ and $\mathbb{K}$ are the standard fourth-order isotropic bulk and shear projection tensors, respectively, κ and μ are the bulk and shear elastic moduli, respectively, and η is the shear viscous modulus. The form of the tensor $\mathbb{H}$ implies that volumetric changes within this phase are purely elastic. Thus, this material response exhibits a single relaxation time given by the ratio $\tau=\eta/\mu$, which, in view of the constitutive relations (1.1), can be written as

$$\frac{\dot{\sigma}_m\mathbf{I}}{3\kappa}+\frac{\dot{\boldsymbol{\sigma}}_d}{2\mu}+\frac{\boldsymbol{\sigma}_d}{2\eta}=\dot{\boldsymbol{\varepsilon}}, \tag{1.5}$$

where $\sigma_m=\mathrm{tr}\boldsymbol{\sigma}/3$ and $\boldsymbol{\sigma}_d=\boldsymbol{\sigma}-\sigma_m\mathbf{I}$ denote the mean and deviatoric parts of $\boldsymbol{\sigma}$, respectively, and $\mathbf{I}$ denotes the second-order identity tensor. In turn, the rigid character of the second phase can be characterized by potentials of the same form (1.3) and (1.4) but with infinitely large elastic and viscous moduli.

The homogenized response relates the macroscopic stress $\overline{\boldsymbol{\sigma}}$ to the macroscopic strain $\overline{\boldsymbol{\varepsilon}}$, which are the averages of the local stress and strain fields, respectively, over the representative volume element subject to appropriate boundary conditions. This relation can be written in terms of the

macroscopic free-energy density and dissipation potential as

$$\overline{\boldsymbol{\sigma}} = \frac{\partial \overline{w}}{\partial \overline{\boldsymbol{\varepsilon}}}(\overline{\boldsymbol{\varepsilon}}, \boldsymbol{\alpha}) \quad \text{and} \quad \frac{\delta \overline{w}}{\delta \boldsymbol{\alpha}(\mathbf{x})}(\overline{\boldsymbol{\varepsilon}}, \boldsymbol{\alpha}) + \frac{\delta \overline{\varphi}}{\delta \dot{\boldsymbol{\alpha}}(\mathbf{x})}(\dot{\boldsymbol{\alpha}}) = \mathbf{0}, \tag{1.6}$$

where

$$\overline{w}(\overline{\boldsymbol{\varepsilon}}, \boldsymbol{\alpha}) = \inf_{\boldsymbol{\varepsilon} \in \mathcal{K}(\overline{\boldsymbol{\varepsilon}})} \langle w(\mathbf{x}, \boldsymbol{\varepsilon}, \boldsymbol{\alpha}) \rangle \quad \text{and} \quad \overline{\varphi}(\dot{\boldsymbol{\alpha}}) = \langle \varphi(\mathbf{x}, \dot{\boldsymbol{\alpha}}) \rangle. \tag{1.7}$$

In these expressions, $\mathcal{K}(\overline{\boldsymbol{\varepsilon}})$ is the set of kinematically admissible strain fields with average $\overline{\boldsymbol{\varepsilon}}$, and the δ operator denotes a functional derivative. For the class of material systems considered in this work, the macroscopic potentials can be written as

$$\overline{w}(\overline{\boldsymbol{\varepsilon}}, \boldsymbol{\alpha}) = (1-c) \inf_{\boldsymbol{\varepsilon} \in \mathcal{K}_r(\overline{\boldsymbol{\varepsilon}})} \left\langle \frac{9}{2} \kappa \, \varepsilon_m^2 + \mu \, (\boldsymbol{\varepsilon}_d - \boldsymbol{\alpha})^2 \right\rangle^{(1)} \quad \text{and} \quad \overline{\varphi}(\dot{\boldsymbol{\alpha}}) = (1-c) \, \eta \left\langle \dot{\boldsymbol{\alpha}}^2 \right\rangle^{(1)}, \tag{1.8}$$

where $c = c^{(2)}$ is the volume fraction of the rigid phase and $\mathcal{K}_r$ is the subset of $\mathcal{K}(\overline{\boldsymbol{\varepsilon}})$ such that $\boldsymbol{\varepsilon} = \mathbf{0}$ within that phase, ε_m and $\boldsymbol{\varepsilon}_d$ denote the mean and deviatoric parts of $\boldsymbol{\varepsilon}$, respectively, the square of a second-order tensor $\mathbf{a}^2 = \mathbf{a} \cdot \mathbf{a}$ has been introduced, and the inelastic strain field $\boldsymbol{\alpha}$ is traceless (i.e. $\mathrm{tr}\boldsymbol{\alpha} = 0$). These macroscopic potentials are isotropic functions of their arguments in view of the assumed isotropy of the local potentials and of the microstructure. Furthermore, they inherit the convexity of the local potentials. Thus, homogenization preserves the generalized standard structure of the local response, with the microscopic inelastic strain field playing the role of a macroscopic internal variable albeit of infinite dimension.

The 'transformation field analysis' of Dvorak [3] simplifies the macroscopic description by assuming uniform inelastic strain fields within each phase and thus employing a finite number of macroscopic internal variables (see, for instance, [4]). For the classes of rigidly reinforced solids considered in this work, that assumption amounts to approximating the macroscopic potentials (1.8) by

$$\overline{w}_{TFA}(\overline{\boldsymbol{\varepsilon}}, \overline{\boldsymbol{\alpha}}) = \tfrac{1}{2} \overline{\boldsymbol{\varepsilon}} \cdot \left(\widetilde{\mathbb{L}} - \mathbb{L}' \right) \overline{\boldsymbol{\varepsilon}} + \tfrac{1}{2} (\overline{\boldsymbol{\varepsilon}} - \overline{\boldsymbol{\alpha}}) \cdot \mathbb{L}' (\overline{\boldsymbol{\varepsilon}} - \overline{\boldsymbol{\alpha}}) \quad \text{and} \quad \overline{\varphi}_{TFA}(\dot{\overline{\boldsymbol{\alpha}}}) = \tfrac{1}{2} \dot{\overline{\boldsymbol{\alpha}}} \cdot \mathbb{M}' \dot{\overline{\boldsymbol{\alpha}}}, \tag{1.9}$$

where $\overline{\boldsymbol{\alpha}}$ is an (traceless) overall inelastic strain, and

$$\widetilde{\mathbb{L}} = 3\widetilde{\kappa} \, \mathbb{J} + 2\widetilde{\mu} \, \mathbb{K}, \quad \mathbb{L}' = \frac{2\mu}{(1-c)} \mathbb{K}, \quad \mathbb{M}' = \frac{2\eta}{(1-c)} \mathbb{K}. \tag{1.10}$$

In these expressions, $\widetilde{\kappa}$ and $\widetilde{\mu}$ are the exact effective moduli of the purely elastic composite. The potentials (1.9) are convex and therefore constitute a generalized standard material model. They generate the macroscopic stress–strain relation

$$\frac{\dot{\overline{\sigma}}_m \mathbf{I}}{3\widetilde{\kappa}} + \frac{\dot{\overline{\boldsymbol{\sigma}}}_d}{2\widetilde{\mu}} + \frac{\overline{\boldsymbol{\sigma}}_d}{2\widetilde{\nu}} = \dot{\overline{\boldsymbol{\varepsilon}}} + \frac{\widetilde{\mu} - \mu'}{\widetilde{\nu}} \overline{\boldsymbol{\varepsilon}}_d, \tag{1.11}$$

where $\widetilde{\nu} = \tau \widetilde{\mu}$ and $\mu' = \mu/(1-c)$. That the transformation field analysis provides overly stiff predictions as repeatedly observed in the literature (e.g. [4]) follows immediately from this relation. Indeed, for any deviatoric deformation applied at a constant rate, for instance, the stress–strain relation (1.11) exhibits linear growth instead of the expected saturation.

An alternative scheme commonly employed in the context of Maxwellian solids consists in approximating the macroscopic response of the composite as Maxwellian (e.g. [5]) and characterizing it by macroscopic potentials of the form

$$\overline{w}_{DS}(\overline{\boldsymbol{\varepsilon}}, \overline{\boldsymbol{\alpha}}) = \tfrac{1}{2} (\overline{\boldsymbol{\varepsilon}} - \overline{\boldsymbol{\alpha}}) \cdot \widetilde{\mathbb{L}} (\overline{\boldsymbol{\varepsilon}} - \overline{\boldsymbol{\alpha}}) \quad \text{and} \quad \overline{\varphi}_{DS}(\dot{\overline{\boldsymbol{\alpha}}}) = \tfrac{1}{2} \dot{\overline{\boldsymbol{\alpha}}} \cdot \widetilde{\mathbb{M}} \dot{\overline{\boldsymbol{\alpha}}}, \tag{1.12}$$

where $\widetilde{\mathbb{L}}$ is still given by $(1.10)_1$ but $\widetilde{\mathbb{M}} = 2\widetilde{\eta}\mathbb{K}$ with $\widetilde{\eta}$ being an effective viscosity. Idiart & Lahellec [6] have shown that this approximation follows from an incremental upper bound that assumes the inelastic strain field is kinematically compatible. The effective elastic moduli follow from the purely elastic homogenization problem while the effective viscosity follows from the purely viscous homogenization problem. Given the mathematical correspondence between these two problems, the effective viscosity of the rigidly reinforced solid can be computed as

$\widetilde{\eta} = \tau \lim_{\kappa\to\infty} \widetilde{\mu}$. Thus, this approximation in effect decouples the viscoelastic homogenization problem and is hence referred to as the 'decoupled scheme'. The potentials (1.12) are convex and therefore constitute a generalized standard material model. They generate the macroscopic stress–strain relation of the same form (1.5), namely

$$\frac{\dot{\overline{\sigma}}_m \mathbf{I}}{3\widetilde{\kappa}} + \frac{\dot{\overline{\boldsymbol{\sigma}}}_d}{2\widetilde{\mu}} + \frac{\overline{\boldsymbol{\sigma}}_d}{2\widetilde{\eta}} = \dot{\overline{\boldsymbol{\varepsilon}}}. \tag{1.13}$$

Unlike the stress–strain relation predicted by the transformation field analysis, this relation is asymptotically exact for small and large time [5], it does exhibit the expected saturation at constant strain rates and can therefore be significantly more accurate. However, it completely neglects macroscopic long-memory effects. An additional purpose of the present study is to assess the merits of the mean-field homogenization scheme presented in the companion paper vis-à-vis this popular decoupled scheme. In the sections that follow we specialize the formulae of the homogenization scheme to rigidly reinforced solids, we then report a collection of sample results for particulate and granular systems and we close with a summary of the findings and some concluding remarks.

2. Mean-field homogenization scheme

In the case of rigidly reinforced solids of interest in this work, the mean-field homogenization scheme of the companion paper generates a reduced-order description in terms of a finite set of effective internal variables given by the volume average of the inelastic strain field and its fluctuations over the viscoelastic phase; we denote those internal variables as

$$\overline{\boldsymbol{\alpha}}^{(1)} = \langle \boldsymbol{\alpha} \rangle^{(1)} \quad \text{and} \quad \widetilde{\alpha}^{(1)} = \left\langle (\boldsymbol{\alpha} - \langle \boldsymbol{\alpha} \rangle^{(1)})^2 \right\rangle^{(1)}, \tag{2.1}$$

respectively. The reduced free-energy density and dissipation potential follow from suitable specialization of the expressions for material systems with isotropic Kelvin–Voigt phases provided in §4 of the companion paper. This specialization is carried out below for elastically compressible systems first and for incompressible systems next.

(a) Elastically compressible systems

The reduced free-energy density and dissipation potential take the respective forms

$$\hat{w}\left(\overline{\boldsymbol{\varepsilon}}, \overline{\boldsymbol{\alpha}}^{(1)}, \widetilde{\alpha}^{(1)}\right) = (1-c) \inf_{\boldsymbol{\varepsilon} \in \mathcal{K}_r(\overline{\boldsymbol{\varepsilon}})} \left[\frac{9}{2} \kappa \, \overline{\overline{\varepsilon}}_m^{(1)^2} + \mu \left(\overline{\boldsymbol{\varepsilon}}_d^{(1)} - \overline{\boldsymbol{\alpha}}^{(1)} \right)^2 + \mu \left(\widetilde{\varepsilon}_d^{(1)} - \widetilde{\alpha}^{(1)} \right)^2 \right] \tag{2.2}$$

and

$$\hat{\varphi}\left(\dot{\overline{\boldsymbol{\alpha}}}^{(1)}, \dot{\widetilde{\alpha}}^{(1)}\right) = (1-c)\, \eta \left[\dot{\overline{\boldsymbol{\alpha}}}^{(1)^2} + \dot{\widetilde{\alpha}}^{(1)^2} \right], \tag{2.3}$$

where

$$\overline{\overline{\varepsilon}}_m^{(1)} = \langle \varepsilon_m^2 \rangle^{(1)\,1/2}, \quad \overline{\boldsymbol{\varepsilon}}_d^{(1)} = \langle \boldsymbol{\varepsilon}_d \rangle^{(1)}, \quad \widetilde{\varepsilon}_d^{(1)} = \left(\langle \boldsymbol{\varepsilon}_d^2 \rangle^{(1)} - \langle \boldsymbol{\varepsilon}_d \rangle^{(1)\,2} \right)^{1/2} \tag{2.4}$$

denote various moments of the mean and deviatoric parts of the strain field over the viscoelastic phase. It is recalled that the kinematic balance $\overline{\boldsymbol{\varepsilon}} = c^{(1)} \overline{\boldsymbol{\varepsilon}}^{(1)} + c^{(2)} \overline{\boldsymbol{\varepsilon}}^{(2)}$ and the requirement of vanishing strain in the rigid phase imply the kinematic relation $\overline{\boldsymbol{\varepsilon}}^{(1)} = \overline{\boldsymbol{\varepsilon}}/(1-c)$ regardless of the microstructural arrangement. These reduced macroscopic potentials generate the constitutive relation

$$\overline{\boldsymbol{\sigma}} = \frac{\partial \hat{w}}{\partial \overline{\boldsymbol{\varepsilon}}} \left(\overline{\boldsymbol{\varepsilon}}, \overline{\boldsymbol{\alpha}}^{(1)}, \widetilde{\alpha}^{(1)} \right) \tag{2.5}$$

along with the evolution laws

$$\tau \dot{\overline{\boldsymbol{\alpha}}}^{(1)} + \overline{\boldsymbol{\alpha}}^{(1)} = \frac{1}{1-c} \overline{\boldsymbol{\varepsilon}}_d \quad \text{and} \quad \tau \dot{\widetilde{\alpha}}^{(1)} + \widetilde{\alpha}^{(1)} = \widetilde{\varepsilon}_d^{(1)} \tag{2.6}$$

for the effective internal variables.

The above expressions require the evaluation of the minimization problem in the reduced free-energy density (2.2). As discussed in the companion paper, this minimization problem can be rewritten as a stationary problem of the form

$$\hat{w}_0(\overline{\boldsymbol{\varepsilon}}, \boldsymbol{\tau}_0, \mu_0) = (1-c) \underset{\boldsymbol{\varepsilon} \in \mathcal{K}_r(\overline{\boldsymbol{\varepsilon}})}{\operatorname{stat}} \left[\frac{9}{2} \kappa \langle \varepsilon_m^2 \rangle^{(1)} + \mu_0 \langle \boldsymbol{\varepsilon}_d^2 \rangle^{(1)} + \boldsymbol{\tau}_0 \cdot \overline{\boldsymbol{\varepsilon}}_d^{(1)} \right] \tag{2.7}$$

$$= (1-c) \underset{\boldsymbol{\varepsilon} \in \mathcal{K}_r(\overline{\boldsymbol{\varepsilon}})}{\operatorname{stat}} \left[\frac{9}{2} \kappa \langle \varepsilon_m^2 \rangle^{(1)} + \mu_0 \langle \boldsymbol{\varepsilon}_d^2 \rangle^{(1)} \right] + \boldsymbol{\tau}_0 \cdot \overline{\boldsymbol{\varepsilon}}_d$$

$$= \frac{9}{2} \widetilde{\kappa}_0 \overline{\varepsilon}_m^2 + \widetilde{\mu}_0 \overline{\boldsymbol{\varepsilon}}_d^2 + \boldsymbol{\tau}_0 \cdot \overline{\boldsymbol{\varepsilon}}_d \tag{2.8}$$

with

$$\boldsymbol{\tau}_0 = 2\mu \left(\frac{\widetilde{\alpha}^{(1)}}{\widetilde{\varepsilon}_d^{(1)}} \overline{\boldsymbol{\varepsilon}}_d^{(1)} - \overline{\boldsymbol{\alpha}}^{(1)} \right) \quad \text{and} \quad \mu_0 = \mu \left(1 - \frac{\widetilde{\alpha}^{(1)}}{\widetilde{\varepsilon}_d^{(1)}} \right), \tag{2.9}$$

where $\widetilde{\kappa}_0$ and $\widetilde{\mu}_0$ are the effective bulk and shear moduli, respectively, of a rigidly reinforced elastic solid with the same microstructure as the original solid and with matrix properties κ and μ_0. The tensor $\boldsymbol{\tau}_0$ plays the role of a stress polarization and should not be confused with a relaxation time. It is easy to show that the strain fields satisfying the minimization conditions in (2.2) and stationarity conditions in (2.7) agree exactly. But it is now readily seen that the computation of the comparison energy (2.7) can be carried out using any mean-field homogenization technique suitable for linearly elastic composites with the microstructure at hand. Indeed, the well-known identities

$$\langle \boldsymbol{\varepsilon}_m^2 \rangle^{(1)} = \frac{1}{(1-c)} \frac{2}{9} \frac{\partial \hat{w}_0}{\partial \kappa}(\overline{\boldsymbol{\varepsilon}}) \quad \text{and} \quad \langle \boldsymbol{\varepsilon}_d^2 \rangle^{(1)} = \frac{1}{(1-c)} \frac{\partial \hat{w}_0}{\partial \mu_0}(\overline{\boldsymbol{\varepsilon}}) \tag{2.10}$$

for the second moments of the strain field imply the identity

$$\widetilde{\varepsilon}_d^{(1)} = \frac{1}{1-c} \left[\frac{9}{2}(1-c) \frac{\partial \widetilde{\kappa}_0}{\partial \mu_0} \overline{\varepsilon}_m^2 + \left((1-c) \frac{\partial \widetilde{\mu}_0}{\partial \mu_0} - 1 \right) \overline{\boldsymbol{\varepsilon}}_d^2 \right]^{1/2} \tag{2.11}$$

for the intraphase strain fluctuations, which taken in combination with $(2.9)_2$ generates a nonlinear equation

$$\left(1 - \frac{\mu_0}{\mu} \right)^2 \left[\frac{9}{2}(1-c) \frac{\partial \widetilde{\kappa}_0}{\partial \mu_0} \overline{\varepsilon}_m^2 + \left((1-c) \frac{\partial \widetilde{\mu}_0}{\partial \mu_0} - 1 \right) \overline{\boldsymbol{\varepsilon}}_d^2 \right] = (1-c)^2 \, \widetilde{\alpha}^{(1)^2} \tag{2.12}$$

for the comparison modulus μ_0. It is noted that this comparison modulus should be such that $\mu_0 \leq \mu$ so that it entails positive strain fluctuations through relation $(2.9)_2$; the sign of μ_0, on the other hand, is unrestricted. The functional dependence of the effective moduli $\widetilde{\kappa}_0$ and $\widetilde{\mu}_0$ on μ_0 follows from the linear elastic homogenization procedure of choice. In general, the algebraic equation (2.12) requires numerical treatment. Whenever it exhibits multiple roots, the root providing the minimum value of the reduced free-energy density (2.2) should be selected. Once μ_0 is determined from this equation, the second moments of the strain field follow from the identities (2.10), the reduced free-energy density follows immediately from (2.2) and the macroscopic constitutive relation can then be obtained by differentiation through (2.5). Alternatively, it can be obtained by differentiation of (2.7) in view of the exact coincidence of the underlying strain fields. This last differentiation must be taken with respect to $\overline{\boldsymbol{\varepsilon}}$, keeping the comparison properties μ_0 and $\boldsymbol{\tau}_0$ fixed, thus generating the expression

$$\overline{\boldsymbol{\sigma}} = 3\widetilde{\kappa}_0 \overline{\varepsilon}_m \mathbf{I} + 2\widetilde{\mu}_0 \overline{\boldsymbol{\varepsilon}}_d + 2\mu \left(\frac{1}{1-c} \frac{\mu - \mu_0}{\mu} \overline{\boldsymbol{\varepsilon}}_d - \overline{\boldsymbol{\alpha}}^{(1)} \right), \tag{2.13}$$

where use has been made of the relation $(2.9)_2$ to eliminate the field fluctuations in favour of μ_0. Knowledge of the strain statistics over the viscoelastic phase also permits the computation of the

corresponding stress statistics, making use of the identities

$$\overline{\sigma}_m^{(1)} = 3\kappa \frac{\overline{\varepsilon}_m}{(1-c)}, \quad \widetilde{\overline{\sigma}}_m^{(1)} = 3\kappa\, \widetilde{\overline{\varepsilon}}_m^{(1)}, \quad \overline{\boldsymbol{\sigma}}_d^{(1)} = 2\mu \left(\overline{\boldsymbol{\varepsilon}}_d^{(1)} - \overline{\boldsymbol{\alpha}}^{(1)}\right), \quad \widetilde{\sigma}_d^{(1)} = 2\mu \left|\widetilde{\varepsilon}_d^{(1)} - \widetilde{\alpha}^{(1)}\right|, \tag{2.14}$$

which are similarly defined and follow from suitable specialization of expressions provided in the companion paper.

It is recalled that the reduced free-energy density (2.2) is non-convex in the Cartesian product space of macroscopic strains and effective internal variables, and therefore the mean-field homogenization scheme does not preserve the generalized standard structure of the exact constitutive relations. The consequences of this non-convexity on the approximate constitutive relations are discussed in the context of the specific examples considered below. It is noted, however, that the free-energy density was found to attain its convexification within a range delimited by certain conditions involving the fluctuations of the total and inelastic strain fields within the phases. In the present context, these conditions reduce to

$$\widetilde{\varepsilon}_d^{(1)} \geq \widetilde{\alpha}^{(1)} \quad \text{or equivalently} \quad \dot{\widetilde{\alpha}}^{(1)} \geq 0. \tag{2.15}$$

On the other hand, the reduced dissipation potential (2.3) is always convex.

(b) Incompressible systems

Fully explicit formulae result when the viscoelastic phase—and therefore the two-phase composite—is incompressible ($\kappa \to \infty$). In this case, $\overline{\varepsilon}_m = 0$ and $\partial\widetilde{\mu}_0/\partial\mu_0 = \widetilde{\mu}_0/\mu_0 = \widetilde{\mu}/\mu$ in view of the homogeneity of degree 1 of the effective shear moduli of the composite $\widetilde{\mu}$ in μ. Equation (2.12) is thus solved by

$$\frac{\mu_0}{\mu} = 1 \pm \frac{(1-c)\,\widetilde{\alpha}^{(1)}}{\sqrt{(1-c)\widetilde{\mu}/\mu - 1}\,\|\overline{\boldsymbol{\varepsilon}}\|}, \tag{2.16}$$

where $\|\cdot\|$ denotes the Euclidean norm of a second-order tensor. The negative root must be selected in view of the constraint $\mu_0 \leq \mu$. The intraphase strain fluctuations (2.11) are then given by

$$\widetilde{\varepsilon}_d^{(1)} = \frac{\sqrt{(1-c)\widetilde{\mu}/\mu - 1}}{1-c}\,\|\overline{\boldsymbol{\varepsilon}}\|, \tag{2.17}$$

and the reduced free-energy density (2.2) is given by

$$\hat{w}\left(\overline{\boldsymbol{\varepsilon}}, \overline{\boldsymbol{\alpha}}^{(1)}, \widetilde{\alpha}^{(1)}\right) = (1-c)\mu \left[\left(\frac{1}{1-c}\overline{\boldsymbol{\varepsilon}} - \overline{\boldsymbol{\alpha}}^{(1)}\right)^2 + \left(\frac{\sqrt{(1-c)\widetilde{\mu}/\mu - 1}}{1-c}\,\|\overline{\boldsymbol{\varepsilon}}\| - \widetilde{\alpha}^{(1)}\right)^2\right]. \tag{2.18}$$

The reduced dissipation potential, in turn, is still given by (2.3). Finally, the macroscopic constitutive relation (2.13) becomes

$$\overline{\boldsymbol{\sigma}} = 2\widetilde{\mu}\,\overline{\boldsymbol{\varepsilon}} - 2\mu\overline{\boldsymbol{\alpha}}^{(1)} - 2\mu\sqrt{(1-c)\widetilde{\mu}/\mu - 1}\,\widetilde{\alpha}^{(1)}\frac{\overline{\boldsymbol{\varepsilon}}}{\|\overline{\boldsymbol{\varepsilon}}\|} - \overline{p}\mathbf{I}, \tag{2.19}$$

where $\overline{p}$ is the macroscopic pressure, and the evolution laws (2.6) for the effective internal variables become

$$\tau\dot{\overline{\boldsymbol{\alpha}}}^{(1)} + \overline{\boldsymbol{\alpha}}^{(1)} = \frac{1}{1-c}\overline{\boldsymbol{\varepsilon}} \quad \text{and} \quad \tau\dot{\widetilde{\alpha}}^{(1)} + \widetilde{\alpha}^{(1)} = \frac{\sqrt{(1-c)\widetilde{\mu}/\mu - 1}}{1-c}\,\|\overline{\boldsymbol{\varepsilon}}\|. \tag{2.20}$$

Thus, the macroscopic viscoelastic response is fully characterized by the effective shear modulus $\widetilde{\mu}$ only.

For later reference, it is noted that the evolution laws (2.20) can be used to express the macroscopic constitutive relation (2.19) in terms of the rates of the internal variables as

$$\overline{\boldsymbol{\sigma}} = 2\eta \left(\dot{\overline{\boldsymbol{\alpha}}}^{(1)} + \sqrt{(1-c)\widetilde{\mu}/\mu - 1}\, \dot{\widetilde{\alpha}}^{(1)} \frac{\overline{\boldsymbol{\varepsilon}}}{\|\overline{\boldsymbol{\varepsilon}}\|} \right) - \overline{p}\mathbf{I}. \tag{2.21}$$

Together with the rate form of the macroscopic constitutive relation (2.19), this expression implies an additive composition of the macroscopic strain rate of the form

$$\frac{\dot{\overline{\boldsymbol{\sigma}}}_d}{2\widetilde{\mu}} + \frac{\overline{\boldsymbol{\sigma}}_d}{2\widetilde{\eta}} = \dot{\overline{\boldsymbol{\varepsilon}}} - \frac{\sqrt{(1-c)\widetilde{\mu}/\mu - 1}}{\widetilde{\mu}/\mu} \widetilde{\alpha}^{(1)} \left[\frac{\dot{\overline{\boldsymbol{\varepsilon}}}}{\|\overline{\boldsymbol{\varepsilon}}\|} \right], \tag{2.22}$$

where $\widetilde{\eta} = \tau\ \widetilde{\mu}$, and $[\dot{\cdot}]$ denotes time differentiation of the quantity inside the square brackets.

3. Results for particulate systems

For illustrative purposes, results are reported in this section for solids reinforced by a special class of rigid dispersions whose effective elastic moduli are given by the Hashin–Shtrikman formalism as (e.g. [7])

$$\widetilde{\kappa} = \kappa + \frac{c}{1-c}\frac{3\kappa+4\mu}{3} \quad \text{and} \quad \widetilde{\mu} = \mu + \frac{5}{2}\frac{c}{1-c}\frac{3\kappa+4\mu}{3\kappa+6\mu}\mu. \tag{3.1}$$

These are material systems of the particulate type whose effective viscoelastic response has been determined exactly by Ricaud & Masson [8] via the correspondence principle of Mandel [9]. Thus, this class provides a suitable benchmark to assess the accuracy of the mean-field homogenization scheme. The exact response is given by

$$\overline{\boldsymbol{\sigma}} = 3\widetilde{\kappa}_1 \overline{\varepsilon}_m \mathbf{I} + 3\widetilde{\kappa}_2(\overline{\varepsilon}_m - \beta_m)\mathbf{I} + 2\widetilde{\mu}_1 \left(\overline{\boldsymbol{\varepsilon}}_d - \boldsymbol{\beta}_1\right) + 2\widetilde{\mu}_2 \left(\overline{\boldsymbol{\varepsilon}}_d - \boldsymbol{\beta}_2\right), \tag{3.2}$$

where the variables β_m and (traceless) $\boldsymbol{\beta}_i$ are initially zero and solve the evolution laws

$$\tau_1 \dot{\beta}_m + \beta_m = \overline{\varepsilon}_m, \quad \tau_1 \dot{\boldsymbol{\beta}}_1 + \boldsymbol{\beta}_1 = \overline{\boldsymbol{\varepsilon}}_d \quad \text{and} \quad \tau_2 \dot{\boldsymbol{\beta}}_2 + \boldsymbol{\beta}_2 = \overline{\boldsymbol{\varepsilon}}_d, \tag{3.3}$$

the moduli $\widetilde{\kappa}_i$ and $\widetilde{\mu}_i$ are given by

$$\widetilde{\kappa}_1 = \frac{1}{1-c}\kappa, \quad \widetilde{\kappa}_2 = \frac{4}{3}\frac{c}{1-c}\mu, \quad \widetilde{\mu}_1 = \mu + \frac{5}{3}\frac{c}{1-c}\mu \quad \text{and} \quad \widetilde{\mu}_2 = \frac{5}{6}\frac{c}{1-c}\frac{\kappa}{\kappa+2\mu}\mu \tag{3.4}$$

and the relaxation times τ_i are given by

$$\tau_1 = \tau \quad \text{and} \quad \tau_2 = \frac{\kappa+2\mu}{\kappa}\tau. \tag{3.5}$$

Thus, this macroscopic response exhibits a discrete spectrum with two relaxation times. It is noted that $\widetilde{\kappa} = \widetilde{\kappa}_1 + \widetilde{\kappa}_2$ and $\widetilde{\mu} = \widetilde{\mu}_1 + \widetilde{\mu}_2$, so that the macroscopic constitutive relation (3.2) can alternatively be written as

$$\overline{\boldsymbol{\sigma}} = 3\widetilde{\kappa}\overline{\varepsilon}_m \mathbf{I} + 2\widetilde{\mu}\overline{\boldsymbol{\varepsilon}}_d - 3\widetilde{\kappa}_2\beta_m\mathbf{I} - 2\widetilde{\mu}_1\boldsymbol{\beta}_1 - 2\widetilde{\mu}_2\boldsymbol{\beta}_2. \tag{3.6}$$

It is also noted that, even though exact, the above formulae do not reveal the physical meaning of the internal variables and their relationship to the microscopic internal variable fields.

For later reference, two special cases are spelled out in further detail. First, we consider the limiting case of incompressible specimens ($\kappa \to \infty$) under isochoric loadings. In this case, the macroscopic mean strain $\overline{\varepsilon}_m$ and the variable β_m vanish identically, the two variables $\boldsymbol{\beta}_1$ and $\boldsymbol{\beta}_2$

follow the same evolution law

$$\tau\dot{\boldsymbol{\beta}} + \boldsymbol{\beta} = \overline{\boldsymbol{\varepsilon}} \tag{3.7}$$

and are therefore identical, and the constitutive relation (3.6) can then be written as

$$\frac{\dot{\overline{\boldsymbol{\sigma}}}_d}{2\widetilde{\mu}} + \frac{\overline{\boldsymbol{\sigma}}_d}{2\widetilde{\eta}} = \dot{\overline{\boldsymbol{\varepsilon}}}, \tag{3.8}$$

where

$$\widetilde{\mu} = \frac{1 + (3/2)c}{1 - c}\mu \quad \text{and} \quad \widetilde{\eta} = \tau\widetilde{\mu} \tag{3.9}$$

represent the effective modulus of elasticity and viscosity of the composite; here, use has been made of the evolution law (3.7) to eliminate the variables $\boldsymbol{\beta}_1 = \boldsymbol{\beta}_2 = \boldsymbol{\beta}$. Second, we consider elastically compressible specimens under spherical loadings. In this case, the variables $\boldsymbol{\beta}_1$ and $\boldsymbol{\beta}_2$ vanish identically, and the evolution law $(3.3)_1$ can be used together with the rate form of (3.6) to eliminate β_m from that expression to obtain

$$\frac{\dot{\overline{\sigma}}_m}{3\widetilde{\kappa}} + \frac{\overline{\sigma}_m}{3\widetilde{\chi}} = \dot{\overline{\varepsilon}}_m + \frac{\widetilde{\kappa} - \widetilde{\kappa}_2}{\widetilde{\chi}}\overline{\varepsilon}_m, \tag{3.10}$$

where $\widetilde{\chi} = \tau\widetilde{\kappa}$.

(a) Estimates for incompressible specimens under isochoric radial deformations

We begin by considering incompressible specimens subject to deformation programmes of the form $\overline{\boldsymbol{\varepsilon}}(t) = \overline{\varepsilon}(t)\mathbf{u}$ with $\|\mathbf{u}\| = 1$, $\mathrm{tr}\mathbf{u} = 0$, and $\overline{\varepsilon}(t)$ such that $\overline{\varepsilon}(t \le 0) = 0$. In this case, the reduced constitutive relation (2.19) and evolution laws (2.20) become

$$\overline{\sigma} = 2\widetilde{\mu}\,\overline{\varepsilon} - 2\mu\,\overline{\alpha}^{(1)} - \mu\sqrt{6c}\,\widetilde{\alpha}^{(1)}\mathrm{sgn}(\overline{\varepsilon}) \tag{3.11}$$

and

$$\tau\dot{\overline{\alpha}}^{(1)} + \overline{\alpha}^{(1)} = \frac{1}{1 - c}\overline{\varepsilon} \quad \text{and} \quad \tau\dot{\widetilde{\alpha}}^{(1)} + \widetilde{\alpha}^{(1)} = \frac{\sqrt{(3/2)c}}{1 - c}|\overline{\varepsilon}|, \tag{3.12}$$

and the statistics (2.14) of the deviatoric stress field in the matrix phase are given by

$$\overline{\sigma}^{(1)} = 2\mu\left(\frac{1}{1 - c}\,\overline{\varepsilon} - \overline{\alpha}^{(1)}\right) \quad \text{and} \quad \widetilde{\sigma}_d^{(1)} = 2\mu\left|\frac{\sqrt{(3/2)c}}{1 - c}|\overline{\varepsilon}| - \widetilde{\alpha}^{(1)}\right|. \tag{3.13}$$

In these expressions, $\overline{\sigma}$, $\overline{\sigma}^{(1)}$ and $\overline{\alpha}^{(1)}$ are the projections of the corresponding tensors onto $\mathbf{u}$. In turn, these relations imply the corresponding specialization of the additive composition (2.22). For any deformation programme $\overline{\varepsilon}(t > 0)$ vanishing at a finite set of time instants only, say t_z with $z = 1, \ldots, Z$, that composition becomes

$$\frac{\dot{\overline{\sigma}}}{2\widetilde{\mu}} + \frac{\overline{\sigma}}{2\widetilde{\eta}} = \left[1 - 2\frac{\sqrt{(1 - c)\widetilde{\mu}/\mu - 1}}{\widetilde{\mu}/\mu}\widetilde{\alpha}^{(1)}\sum_{z=1}^{Z}\frac{\delta(t - t_z)}{|\dot{\overline{\varepsilon}}(t_z)|}\right]\dot{\overline{\varepsilon}}(t), \tag{3.14}$$

where $\widetilde{\mu}$ and $\widetilde{\eta}$ are given by (3.9), the function $\delta(\cdot)$ denotes a Dirac mass and the identity should be understood in the sense of distributions.

Figure 1*a* displays the exact material response for a specimen with $c = 0.25$ subject to a triangular signal $\overline{\varepsilon}(t)$ of amplitude γ_0 and period $4T_0$ with $T_0 = 20\tau$, along with the response predicted by the reduced homogenization scheme—also referred to as the 'effective internal variable' (EIV) scheme—and the response of the unreinforced matrix phase, normalized by γ_0 and $\sigma_0 = 2\eta\gamma_0/T_0$. The various responses are computed numerically by integrating in time expressions (3.8), (3.11) and (3.12) using an implicit Euler scheme with uniform time step. This is a very special case for which the decoupled scheme (1.13) recovers the exact response (3.8). We begin by noting that the reduced estimates recover the exact response during the first half-cycle of the deformation programme. This is confirmed analytically by comparing expression (3.14) with expression (3.8): during the open time interval $(0, T_0)$ the second term within the square brackets

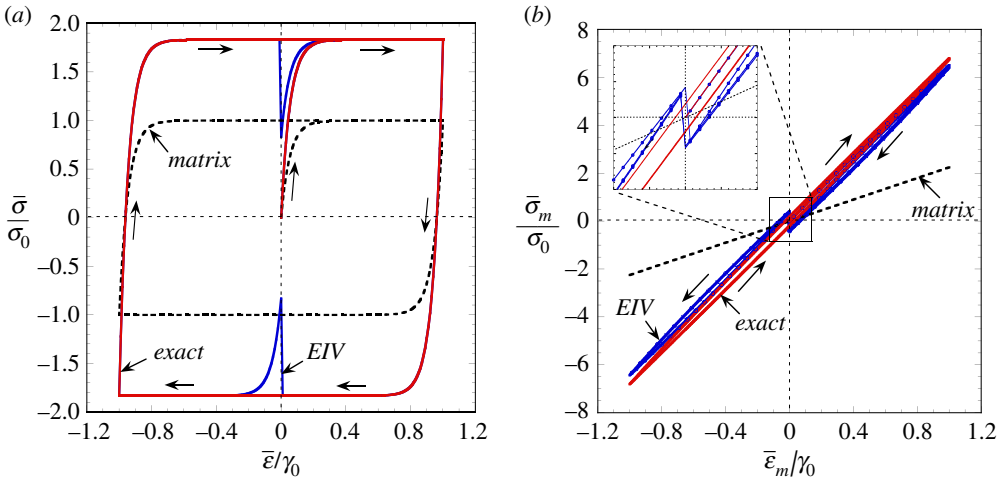

Figure 1. Predictions for particulate solids with $c = 0.25$ subject to triangular signals with period $4T_0$: (*a*) macroscopic deviatoric response of an incompressible solid under a signal with $T_0 = 20\tau$; (*b*) macroscopic spherical response of a compressible solid with $\kappa = 2\mu$ under a signal with $T_0 = 1.5\tau$. (Online version in colour.)

in (3.14) is identically zero and both expressions coincide. Interestingly, this is despite the fact that the convexity conditions (2.15) cease to hold soon after unloading begins to take place. In turn, this suggests that such conditions do not constitute a precise delimiter for the range of validity of the reduced-order approximation. Beyond the first half-cycle, however, the exact response remains saturated until further reloading while the reduced estimates exhibit a spurious transient when the strain fluctuations $\widetilde{\varepsilon}_d^{(1)}$ vanish. During this transient the reduced estimates predict a stress level for the composite that is even smaller than that sustained by the unreinforced matrix, thus violating elementary lower bounds. In fact, the reduced estimates exhibit such a transient every time the applied deformation vanishes. Similar transients have already been reported by Boudet *et al.* [10] and Lucchetta *et al.* [11] in the context of elastoplastic composites. The analytical source of these transients is clearly seen in the above formulae: the sign function in expression (3.11) and the delta functions in expression (3.14). The source of these offending terms, in turn, can be traced to the non-convexity of the reduced free-energy density already identified in the companion paper. Indeed, for radial deformation programmes the reduced free-energy (2.18) takes the form

$$\hat{w}\left(\overline{\varepsilon}\mathbf{u}, \overline{\alpha}^{(1)}\mathbf{u}, \widetilde{\alpha}^{(1)}\right) = \frac{\mu}{1-c}\left[\left(\overline{\varepsilon} - (1-c)\overline{\alpha}^{(1)}\right)^2 + \left(\sqrt{(3/2)c}\,|\overline{\varepsilon}| - (1-c)\widetilde{\alpha}^{(1)}\right)^2\right]. \tag{3.15}$$

This function is non-convex on the entire Cartesian product space of $\overline{\varepsilon}$, $\overline{\alpha}^{(1)}$ and $\widetilde{\alpha}^{(1)}$; however, it is convex on the subspaces with $\overline{\varepsilon}$ of constant sign. On the other hand, if this non-convex free-energy density is replaced by the convex density

$$\hat{w}\left(\overline{\varepsilon}\mathbf{u}, \overline{\alpha}^{(1)}\mathbf{u}, \widetilde{\alpha}^{(1)}\right) = \frac{\mu}{1-c}\left[\left(\overline{\varepsilon} - (1-c)\overline{\alpha}^{(1)}\right)^2 + \left(\sqrt{(3/2)c}\,\overline{\varepsilon} - (1-c)\widetilde{\alpha}^{(1)}\right)^2\right], \tag{3.16}$$

keeping the reduced dissipation potential (2.3) and reinterpreting the effective internal variable $\widetilde{\alpha}^{(1)}$ as a signed quantification of the inelastic strain fluctuations so that it is allowed to become negative, the spurious transients no longer occur and the exact response for general deformation programmes $\overline{\varepsilon}(t)$ is obtained. This replacement of the reduced free-energy density—henceforth referred to as 'convexification'—is equivalent to the algorithmic correction devised by Idiart & Lahellec [6], Boudet *et al.* [10] and Lucchetta *et al.* [11] on the basis of exploiting the existence of multiple stationary points in the approximate incremental functionals of Lahellec & Suquet [1,12]. Unfortunately, this remedy can only be carried out when the strain fluctuations are strictly

proportional to the applied deformation. In any case, it is interesting to note that the potentials (3.16) and (2.3) are thus seen to constitute the generalized standard structure of the exact relations of Ricaud & Masson [8] in this case. The connection between the variables $\boldsymbol{\beta}_i$ employed in those relations and the effective internal variables employed in the 'convexified' estimates is

$$\boldsymbol{\beta}_1 = (1-c)\overline{\alpha}^{(1)}\mathbf{u} \equiv (1-c)\overline{\boldsymbol{\alpha}}^{(1)} \quad \text{and} \quad \boldsymbol{\beta}_2 = \frac{1-c}{\sqrt{(3/2)c}}\widetilde{\alpha}^{(1)}\mathbf{u} \equiv \frac{\widetilde{\alpha}^{(1)}}{\widetilde{\varepsilon}^{(1)}}\overline{\boldsymbol{\varepsilon}}, \tag{3.17}$$

where $\widetilde{\varepsilon}^{(1)}$ should be understood as a signed quantification of the strain fluctuations within the matrix phase. This follows from introducing these relations into the evolution laws (3.7) for the variables $\boldsymbol{\beta}_i$ and verifying that the 'convexified' evolution laws for the variables $\overline{\alpha}^{(1)}$ and $\widetilde{\alpha}^{(1)}$ are obtained. Thus, $\boldsymbol{\beta}_1$ is the average inelastic strain, and $\boldsymbol{\beta}_2$ is the average strain weighted by the ratio of inelastic strain to total strain fluctuations. This is in contrast to the effective internal variables (2.1) employed by the mean-field homogenization scheme, which represent intraphase statistics of the inelastic strain field only.

(b) Estimates for compressible specimens under spherical deformations

We now consider compressible specimens subject to spherical deformation programmes of the form $\overline{\boldsymbol{\varepsilon}}(t) = \overline{\varepsilon}_m(t)\mathbf{I}$ with $\overline{\varepsilon}_m(t \le 0) = 0$. In this case, the effective internal variable $\overline{\boldsymbol{\alpha}}^{(1)}$ vanishes identically throughout the deformation process and the dissipation is entirely due to $\widetilde{\alpha}^{(1)}$, whose evolution depends on μ_0. Recalling that $\widetilde{\kappa}_0$ is given by expression $(3.1)_1$ with μ replaced by μ_0, equation (2.12) for μ_0 reduces to

$$\left(1 - \frac{\mu_0}{\mu}\right)^2 6\,c\,\overline{\varepsilon}_m^2 = (1-c)^2\,\widetilde{\alpha}^{(1)^2}, \tag{3.18}$$

which is solved by

$$\frac{\mu_0}{\mu} = 1 - \frac{(1-c)\widetilde{\alpha}^{(1)}}{\sqrt{6\,c}\,|\overline{\varepsilon}_m|} \tag{3.19}$$

within the admissible range $\mu_0 \le \mu$. The reduced constitutive relation (2.13) then becomes

$$\overline{\sigma}_m = 3\widetilde{\kappa}\overline{\varepsilon}_m - \frac{2}{3}\mu\sqrt{6\,c}\,\widetilde{\alpha}^{(1)}\,\mathrm{sgn}(\overline{\varepsilon}_m), \tag{3.20}$$

while the evolution law (2.6) for $\widetilde{\alpha}^{(1)}$ becomes

$$\tau\dot{\widetilde{\alpha}}^{(1)} + \widetilde{\alpha}^{(1)} = \frac{\sqrt{6\,c}}{1-c}\,|\dot{\overline{\varepsilon}}_m|. \tag{3.21}$$

In turn, the non-trivial statistics (2.14) of the stress field within the matrix phase are given by

$$\overline{\overline{\sigma}}_m^{(1)} = 3\kappa\frac{|\overline{\varepsilon}_m|}{(1-c)} \quad \text{and} \quad \widetilde{\sigma}_d^{(1)} = 2\mu\left|\frac{\sqrt{6c}}{1-c}|\overline{\varepsilon}_m| - \widetilde{\alpha}^{(1)}\right|. \tag{3.22}$$

For any deformation programme $\overline{\varepsilon}_m(t > 0)$ vanishing at a finite set of time instants only, say t_z with $z = 1, \ldots, Z$, these relations imply that

$$\frac{\dot{\overline{\sigma}}_m}{3\widetilde{\kappa}} + \frac{\overline{\sigma}_m}{3\widetilde{\chi}} = \left[1 - \sqrt{6c}\,\frac{4\mu}{9\widetilde{\kappa}}\widetilde{\alpha}^{(1)}\sum_{z=1}^{Z}\frac{\delta(t-t_z)}{|\dot{\overline{\varepsilon}}_m(t_z)|}\right]\dot{\overline{\varepsilon}}_m + \frac{\widetilde{\kappa} - \widetilde{\kappa}_2}{\widetilde{\chi}}\overline{\varepsilon}_m, \tag{3.23}$$

where $\widetilde{\chi} = \tau\widetilde{\kappa}$.

The fact that the structure of these formulae resembles those of incompressible solids obtained in the previous subsection permits a similar analysis. Figure 1*b* displays the exact material response of a specimen with $\kappa = 2\mu$ and $c = 0.25$ subject to a triangular signal $\overline{\varepsilon}_m(t)$ of amplitude γ_0 and period $4T_0$ with $T_0 = 1.5\tau$, along with the response predicted by the reduced homogenization scheme and the response of the unreinforced matrix phase, normalized by γ_0 and $\sigma_0 = 2\eta\gamma_0/T_0$. The various responses are computed numerically by integrating in time expressions (3.10), (3.20)

and (3.21) using an implicit Euler scheme with uniform time step. Once again, the reduced estimates recover the exact response during the first half-cycle of the deformation programme. This can be confirmed analytically by comparing expression (3.23) with expression (3.10): during the open time interval $(0, T_0)$ the second term within the square brackets in (3.23) is identically zero and both expressions coincide. Up to that point, the reduced estimates are thus able to capture the correct contribution of local dissipation to the macroscopic spherical response. We note in passing that this is in contrast to the popular decoupled scheme (1.13)—not shown—which predicts a purely elastic spherical response. Beyond that point, however, the reduced estimates exhibit spurious transients every time the applied deformation vanishes, as a consequence of the sign function in expression (3.20) and the delta functions in expression (3.23). This is yet another manifestation of the non-convexity of the reduced free-energy density. Indeed, making use of (3.19) in (2.9), it is easy to verify that the reduced free-energy density (2.2) is given by

$$\hat{w}\left(\overline{\varepsilon}_m \mathbf{I}, \widetilde{\alpha}^{(1)}\right) = \frac{9}{2}\kappa \frac{\overline{\varepsilon}_m^2}{1-c} + \frac{\mu}{(1-c)}\left(\sqrt{6\,c}\,|\overline{\varepsilon}_m| - (1-c)\widetilde{\alpha}^{(1)}\right)^2. \tag{3.24}$$

This function is non-convex on the entire Cartesian product space of $\overline{\varepsilon}_m$ and $\widetilde{\alpha}^{(1)}$; however, it is convex on the subspaces with $\overline{\varepsilon}_m$ of constant sign. Now, a similar remedy to the one applied in the previous subsection can also be applied in this case. Indeed, if this non-convex free-energy density is replaced by the convex density

$$\hat{w}\left(\overline{\varepsilon}_m \mathbf{I}, \widetilde{\alpha}^{(1)}\right) = \frac{9}{2}\kappa \frac{\overline{\varepsilon}_m^2}{1-c} + \frac{\mu}{(1-c)}\left(\sqrt{6\,c}\,\overline{\varepsilon}_m - (1-c)\widetilde{\alpha}^{(1)}\right)^2, \tag{3.25}$$

keeping the reduced dissipation potential

$$\hat{\varphi}\left(\widetilde{\alpha}^{(1)}\right) = (1-c)\,\eta\,\widetilde{\alpha}^{(1)^2} \tag{3.26}$$

and reinterpreting the effective internal variable $\widetilde{\alpha}^{(1)}$ as a signed quantification of the viscous strain fluctuations—so that it is allowed to become negative—the spurious transients no longer occur and the exact response for general $\overline{\varepsilon}_m(t)$ is obtained. Furthermore, the potentials (3.25) and (3.26) provide the generalized standard structure for the exact relations of Ricaud & Masson [8] in this case. The connection between the variable β_m employed in those relations and the local fields is given by

$$\beta_m = \frac{1-c}{\sqrt{6\,c}}\,\widetilde{\alpha}^{(1)} \equiv \frac{\widetilde{\alpha}^{(1)}}{\widetilde{\varepsilon}^{(1)}}\overline{\varepsilon}_m, \tag{3.27}$$

where $\widetilde{\varepsilon}^{(1)}$ should be understood as a signed quantification of the deviatoric strain fluctuations within the matrix phase. This follows from introducing relation (3.27) into the evolution law $(3.3)_1$ for the variable β_m and verifying that the 'convexified' evolution law for the variable $\widetilde{\alpha}^{(1)}$ is obtained. Thus, β_m is the average spherical strain weighted by the ratio of inelastic strain to deviatoric strain fluctuations.

(c) Estimates for compressible specimens under isochoric complex deformations

We now consider compressible specimens subject to isochoric deformation programmes ($\overline{\varepsilon}_m = 0$) of the form

$$\overline{\boldsymbol{\varepsilon}}(t) = \overline{\varepsilon}_{ss}(t)\,(\mathbf{e}_1 \otimes \mathbf{e}_3 + \mathbf{e}_3 \otimes \mathbf{e}_1) + \overline{\varepsilon}_{as}(t)\left(\mathbf{e}_1 \otimes \mathbf{e}_1 - \tfrac{1}{2}\,\mathbf{e}_2 \otimes \mathbf{e}_2 - \tfrac{1}{2}\,\mathbf{e}_3 \otimes \mathbf{e}_3\right) \tag{3.28}$$

relative to a fixed orthonormal basis $\{\mathbf{e}_i\}$ and a stress-free initial configuration, where the first term corresponds to a simple shear along the axis $\mathbf{e}_1$ and the second term corresponds to an axisymmetric shear about that same axis. Four different programmes are studied, as follows.

PROGRAMME 1. A radial axisymmetric deformation consisting of a linear ramp followed by a sinusoidal signal

$$\overline{\varepsilon}_{ss}(t)=0 \quad \text{and} \quad \overline{\varepsilon}_{as}(t)=\begin{cases}\gamma_0\dfrac{t}{T_0} & 0\le t\le T_0,\\ \gamma_0\left[1+\dfrac{1}{2\pi}\sin\left(2\pi\dfrac{t-T_0}{T_0}\right)\right] & T_0<t.\end{cases} \tag{3.29}$$

PROGRAMME 2. A radial deformation followed by a deformation with rotating principal axes as given by $(3.29)_2$ and

$$\overline{\varepsilon}_{ss}(t)=\begin{cases}\gamma_0\dfrac{t}{T_0} & 0\le t\le T_0,\\ \gamma_0\left[1-\dfrac{1}{2\pi}\left(1-\cos\left(2\pi\dfrac{t-T_0}{T_0}\right)\right)\right] & T_0<t.\end{cases} \tag{3.30}$$

PROGRAMME 3. A radial axisymmetric deformation consisting of a triangular signal given by

$$\overline{\varepsilon}_{ss}(t)=0 \quad \text{and} \quad \overline{\varepsilon}_{as}(t)=\frac{\gamma_0}{T_0}\left(t-2T_0\left\lfloor\frac{t+T_0}{2T_0}\right\rfloor\right)(-1)^{\left\lfloor\frac{t+T_0}{2T_0}\right\rfloor}, \tag{3.31}$$

where $\lfloor x\rfloor=\max\{m\in\mathbb{Z}\mid m\le x\}$ denotes the floor function.

PROGRAMME 4. A deformation with rotating principal axes given by

$$\overline{\varepsilon}_{ss}(t)=\gamma_0\left[1-\cos\left(\frac{2\pi t}{T_0}\right)\right] \quad \text{and} \quad \overline{\varepsilon}_{as}(t)=\gamma_0\sin\left(\frac{2\pi t}{T_0}\right). \tag{3.32}$$

These programmes are characterized by reference deformation and time constants γ_0 and T_0. In all cases, the evolution equations (2.6) with (2.11) are integrated numerically following an implicit Euler scheme with uniform time step. At each time step in the scheme, equation (2.12) must be solved numerically for the comparison modulus μ_0, where $\widetilde{\mu}_0$ is given by expression $(3.1)_2$ with μ replaced by μ_0. During the initial stages of the various deformation programmes, this equation has only one real root in the admissible range $\mu_0\le\mu$, but during some intervals multiple roots appear. In those intervals, it has been verified that the root within the range $-\kappa/2\le\mu_0\le\mu$ always furnishes the minimum value of the reduced free-energy density and must therefore be selected. It can be verified that for this class of composites under isochoric deformations the comparison modulus μ_0 does not depend on reinforcement content c and depends on the macroscopic deformation through the combination $[\|\dot{\overline{\boldsymbol{\varepsilon}}}_d\|]/\|\overline{\boldsymbol{\varepsilon}}_d\|$ only; the comparison modulus is thus a homogeneous function of degree zero in the entire history $\overline{\boldsymbol{\varepsilon}}_d[t]$. We report predictions for specimens with matrix bulk modulus $\kappa=2\mu$ and reinforcement volume fraction $c=0.25$, normalized by γ_0 and $\sigma_0=2\eta\gamma_0/T_0$.

Figure 2 displays the predicted material response under the first deformation programme with $T_0=2\tau$. Also displayed for comparison purposes are the exact response of the reinforced solid and the response of the unreinforced matrix phase. We begin by noting that the reduced estimates (EIV) are in very good agreement with the exact response for the entire programme. Thus, the estimates are seen to capture both the transient and steady-state responses very accurately. This is in line with the earlier comparisons reported in Lahellec & Suquet [1] for cyclic loadings. It is also, once again, despite the fact that the convexity conditions (2.15) cease to hold periodically after the first cycle.

Figure 3 displays the predicted material response under the second deformation programme with $T_0=20\tau$. In contrast to the previous programme, this programme reveals quantitative discrepancies between the reduced estimates and the exact response once the applied deformation ceases to be radial. It is natural to speculate that such discrepancies would be partially due to the use of an isotropic measure of inelastic strain fluctuations $\widetilde{\alpha}^{(1)}$ as an effective internal variable, and that they could be mitigated by using a separate fluctuation measure for each deformation mode, as already mentioned in the companion paper. Unfortunately, this is not

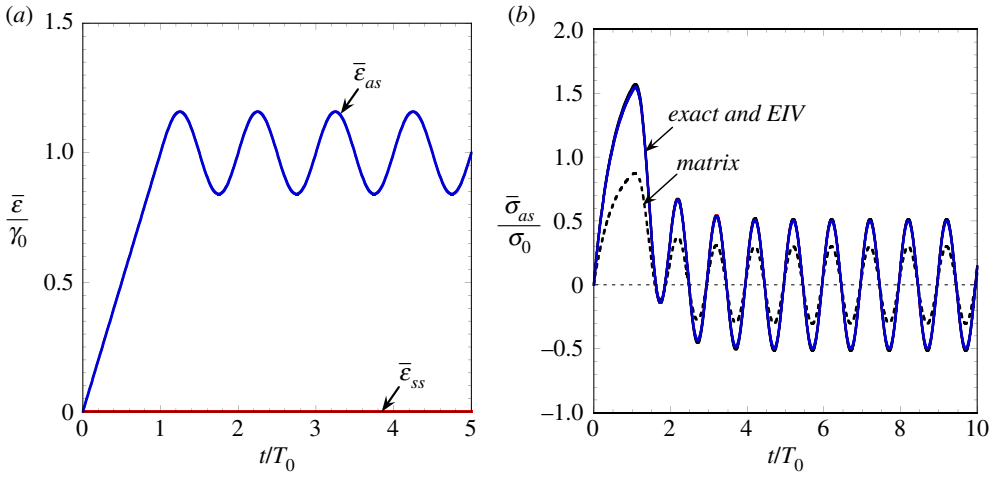

Figure 2. Predictions for particulate solids with $\kappa = 2\mu$ and $c = 0.25$, subject to deformation programme 1 with $T_0 = 2\tau$: (*a*) macroscopic deformation and (*b*) macroscopic stress versus time. (Online version in colour.)

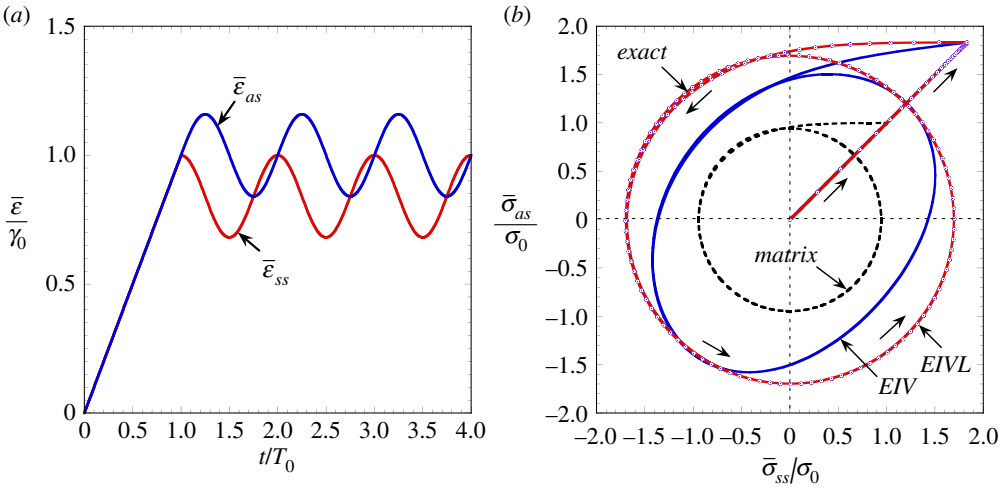

Figure 3. Predictions for particulate solids with $\kappa = 2\mu$ and $c = 0.25$, subject to deformation programme 2 with $T_0 = 20\tau$: (*a*) macroscopic deformation versus time and (*b*) macroscopic stresses. (Online version in colour.)

the case. Results for specimens subject to simultaneous shear and dilatational deformations—omitted here for brevity—display similar discrepancies even though the inelastic strain field is deviatoric. Instead, the discrepancies are a consequence of a spurious non-linearity in the reduced constitutive relations, which is yet another manifestation of the non-convexity of the reduced free-energy density. Thus, *the exact stress response is identically equal to the additive composition of the stress responses produced by each deformation mode in* (3.28) *imposed independently, while the reduced stress response is clearly not, in view of the non-quadratic form of the reduced free-energy density* (2.2). That this is indeed the source of discrepancy can be exposed by generating a linearized version of the reduced estimates, additively composing the stress responses predicted by the mean-field homogenization scheme for each deformation mode applied independently. Such linearized estimates (EIVL) are now seen to be in very good agreement with the exact response for the entire loading programme.

Figure 4 displays the material response under the third deformation programme with $T_0 = 20\tau$. We begin by noting that the reduced estimates are in remarkable agreement with the exact

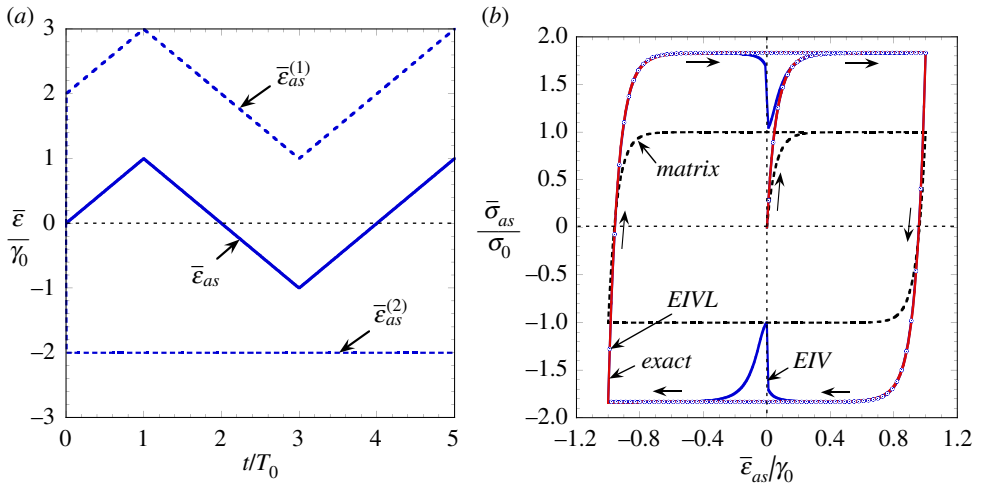

Figure 4. Predictions for particulate solids with $\kappa = 2\mu$ and $c = 0.25$, subject to deformation programme 3 with $T_0 = 20\tau$: (*a*) macroscopic deformation versus time and (*b*) macroscopic response. (Online version in colour.)

response for most part of the programme. In fact, it can be shown that the reduced estimates exhibit the exact initial elastic slope and subsequent viscous plateau. This is in line with the earlier comparisons reported in Lahellec & Suquet [1] for monotonic loadings. However, the estimates also exhibit spurious transients every time the applied deformation vanishes. These are the same transients already identified in the context of incompressible composites as a consequence of the non-convexity of the reduced free-energy density, spread out by matrix compressibility. Unfortunately, the strain fluctuations are not strictly proportional to the applied deformation and consequently the 'convexification' devised in the previous subsections cannot be carried out. However, it is still possible to eliminate the transients by linearizing the reduced estimates as in the previous deformation programme. In this connection, we note that no transients occurred in the first and second deformation programmes considered previously because the norm of the macroscopic strain tensor remained always finite and sufficiently large. Then, the applied deformation $\overline{\varepsilon}_{\rm as}(t)$ can always be expressed as an additive composition of various deformations such that, when applied independently, they produce macroscopic strains with sufficiently large norms to avoid spurious transients. Figure 4*a* shows two such deformation programmes, $\overline{\varepsilon}^{[1]}_{\rm as}(t)$ and $\overline{\varepsilon}^{[2]}_{\rm as}(t)$, whose additive composition produces the original programme (3.31). The additive compositions of the corresponding reduced stresses (EIVL) are now seen to be smooth and in very good agreement with the exact response for the entire deformation programme.

Finally, figure 5 displays the material response under the fourth deformation programme with $T_0 = 20\tau$. As the second deformation programme, this programme reveals quantitative discrepancies between the reduced estimates and the exact response once the applied deformation deviates considerably from a radial history. Unlike the second deformation programme, on the other hand, this programme produces vanishing macroscopic strains at $t = T_0$, $2T_0$, etc. At those instants, the reduced estimates exhibit the spurious transients generated by the non-convexity of the reduced free-energy density already described in the context of radial deformations. Once again, these transients can be eliminated by linearization. Given that both applied deformations $\overline{\varepsilon}_{ss}(t)$ and $\overline{\varepsilon}_{as}(t)$ vanish periodically, both deformations must be expressed as additive compositions of non-vanishing deformations. Figure 5*a* shows two pairs of such deformation programmes $\overline{\varepsilon}^{[1]}_{ss}(t)$, $\overline{\varepsilon}^{[2]}_{ss}(t)$, $\overline{\varepsilon}^{[1]}_{as}(t)$ and $\overline{\varepsilon}^{[2]}_{as}(t)$. The additive compositions of the corresponding pairs of reduced stresses (EIVL) are now seen to be smooth and in very good agreement with the exact response for the entire deformation programme. This linearization procedure emerges then as a plausible alternative to remedy the spurious effects introduced by

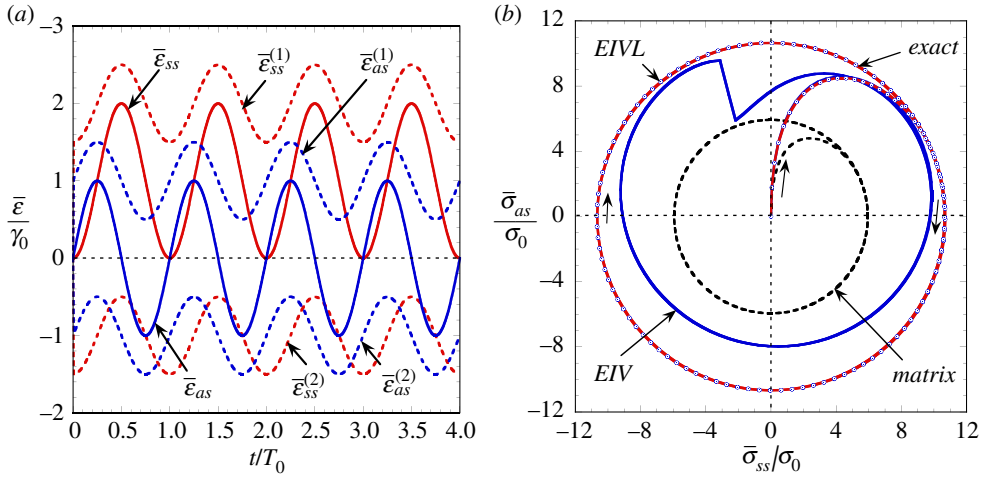

Figure 5. Predictions for particulate solids with $\kappa = 2\mu$ and $c = 0.25$, subject to deformation programme 4 with $T_0 = 20\tau$: (*a*) macroscopic deformation versus time and (*b*) macroscopic stresses. (Online version in colour.)

the non-convexity of the reduced free-energy density. Moreover, the procedure can be used to generate estimates not only for the macroscopic response but also for the first- and second-order intraphase statistics of the microscopic fields. A formal exposition of the procedure is advanced in appendix A.

4. Results for granular systems

We now consider a special class of two-phase granular systems with microgeometries such that their effective elastic moduli are given by the self-consistent formalism as (e.g. [7])

$$\widetilde{\kappa} = \frac{\kappa}{1-c} + \frac{4}{3}\frac{c}{1-c}\widetilde{\mu} \quad \text{and} \quad \widetilde{\mu} = \frac{\mu}{1-c} + \frac{c}{1-c}\frac{9\widetilde{\kappa}+8\widetilde{\mu}}{6\widetilde{\kappa}+12\widetilde{\mu}}\widetilde{\mu}. \tag{4.1}$$

Note that these expressions define the effective moduli implicitly. In the limiting case of incompressible systems ($\kappa \to \infty$), however, the shear modulus is explicitly given by

$$\widetilde{\mu} = \frac{\mu}{1-(5/2)c}. \tag{4.2}$$

Unlike the previous class of particulate systems, this class of granular systems exhibits a macroscopic response with a continuous spectrum [13] and, furthermore, is percolative. The percolation threshold depends on whether the systems are compressible or incompressible: if κ is bounded, percolation occurs at a reinforcement content $c_0 = 0.5$; if κ is unbounded, percolation occurs at the lower reinforcement content $c_0 = 0.4$. At such reinforcement contents, the above moduli become unbounded and the composite is elastically rigid. A few results for this class of granular systems are already available in the literature. For instance, Beurthey & Zaoui [13] have derived the exact relaxation spectrum when both phases are viscoelastic but incompressible, while Laws & McLaughlin [14] have computed approximate results via the collocation method when one of the phases is purely elastic. To the best of our knowledge, no exact analytical description is available for the compressible systems considered here. On the other hand, the reduced estimates can be computed as easily as in the previous case of particulate systems. Once again, the evolution equations (2.6) with (2.11) can be integrated numerically following an implicit Euler scheme with uniform time step. At each time step in the scheme, equation (2.12) must be solved for the comparison modulus μ_0, where $\widetilde{\kappa}_0$ and $\widetilde{\mu}_0$ are given by expressions (4.1) with μ replaced by μ_0. However, given that these self-consistent expressions are not explicit in the effective moduli, it is

more convenient to rewrite them as

$$\widetilde{\kappa}_0 = \frac{1}{1-c}\kappa + \frac{c}{1-c}\frac{4}{3}\widetilde{\mu}_0 \quad \text{and} \quad \mu_0 = \left[1 - \frac{5}{2}c\,\frac{3\kappa + 4\widetilde{\mu}_0}{3\kappa + 2(3-c)\widetilde{\mu}_0}\right]\widetilde{\mu}_0 \tag{4.3}$$

and take $\widetilde{\mu}_0$ as the unknown to be determined numerically rather than μ_0. When the equation exhibits multiple roots, the root such that $-\kappa/2 \le \mu_0 \le \mu$ must be selected. We report below predictions for specimens with $\kappa = 2\mu$, normalized by γ_0 and $\sigma_0 = 2\eta\gamma_0/T_0$.

Figure 6 displays the predicted material responses for specimens under the third deformation programme introduced in the previous section with $T_0 = 20\tau$ and two different reinforcement contents $c = 0.25$ and $c = 0.45$. Also displayed for comparison purposes are the response of the reinforced composite predicted by the decoupled scheme (DS) as given by (1.13) with $\widetilde{\mu}$ given by (4.1), and the response of the unreinforced viscoelastic phase. Several observations are in order. We begin by noting that the reduced estimates (EIV) for both reinforcement contents exhibit the expected behaviour during the initial loading ramp but exhibit the spurious transients already observed in the context of particulate systems, which seem to be exacerbated by the granular microstructures. Once again, these transients can be eliminated by linearly composing the predictions for multiple deformation programmes whose composition is equivalent to the original programme. The linearized estimates reported in the figure were generated with the same deformation programmes displayed in figure 4*a*. However, a deformation step $\overline{\varepsilon}_{as}^{[2]}$ of twice the magnitude was required to eliminate the transients completely. The linearized estimates (EIVL) are now seen to exhibit the expected trends for the entire deformation programmes. At the moderate reinforcement content ($c = 0.25$), the predicted response exhibits the expected saturation but with a more pronounced viscoelastic transition than that observed in particulate systems. This is in contrast to the response predicted by the decoupled scheme, which exhibits a much more abrupt transition as a result of neglecting long-memory effects. At the high reinforcement content ($c = 0.45$), however, these differences between the two schemes are not only quantitative but also qualitative. It is recalled that the effective viscosity of the decoupled scheme can be expressed as $\widetilde{\eta} = \tau \lim_{\kappa\to\infty} \widetilde{\mu}$ and, therefore, exhibits the same percolation threshold as the incompressible shear modulus (4.2). Thus, the decoupled scheme predicts a purely elastic response for any reinforcement content above that percolation threshold. By contrast, the reduced estimates still display dissipative behaviour. This behaviour is seen to exhibit linear growth instead of the typical saturation observed for moderate reinforcement content. Whether these predictions are accurate or not remains to be confirmed via comparisons with full-field numerical simulations. Now, it should be noted that, while certainly auspicious, this linearization procedure requires additional effective internal variables, it may not provide a clear thermodynamic meaning of the approximate constitutive relations and its application to nonlinear rheologies is not straightforward. In any case, the mere fact that it can capture the strong influence of microstructure on macroscopic behaviour and field fluctuations with such a reduced number of effective internal variables is already a positive result, as no other mean-field homogenization method to date seems to share this capacity.

5. Concluding remarks

The capabilities and limitations of the mean-field homogenization scheme of Lahellec & Suquet [1] for viscoelastic composites have been assessed in light of the mathematical structure exposed in the companion paper. The scheme entails in effect a model reduction that identifies effective internal variables with the first moments of the inelastic strain field and its fluctuations over each phase, and therefore endows them with a clear physical meaning. The reduced constitutive behaviour preserves the two-potential structure of the exact constitutive behaviour being approximated but does not preserve its global convexity. Still, the scheme was found to generate highly accurate and even exact descriptions of the macroscopic response whenever stress-free specimens were subject to deformations lying within the convex range of the reduced free-energy density. Beyond that range, predicted responses can remain accurate but can also

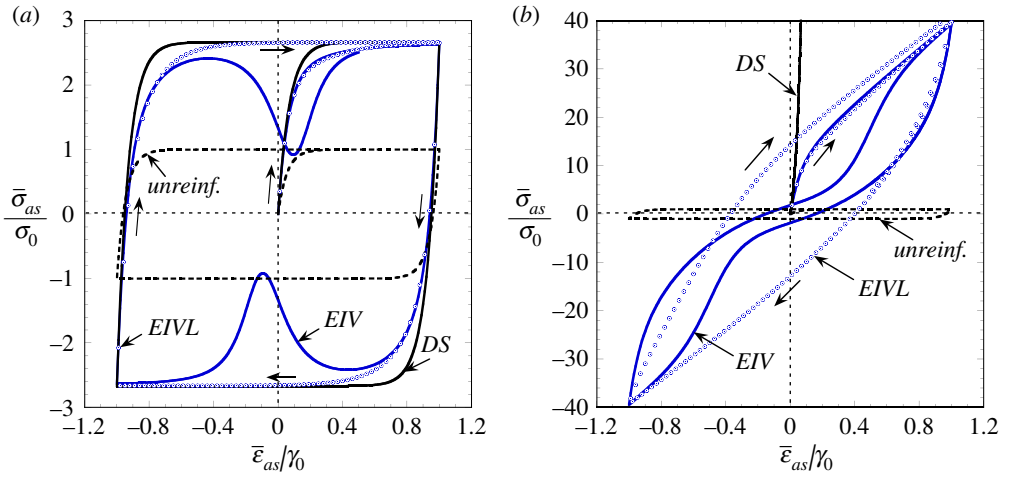

Figure 6. Predictions for granular solids with $\kappa = 2\mu$, subject to deformation programme 3 with $T_0 = 20\tau$: (*a*) macroscopic response for $c = 0.25$, (*b*) macroscopic response for $c = 0.45$. (Online version in colour.)

exhibit spurious transients and non-linearities. In the simplest cases considered, 'convexified' free-energy densities delivering the exact response were realized. In the more general cases, a linearization procedure capable of delivering highly accurate predictions with minimal computational cost was devised. These results pave the way to generating reduced-order models for viscoelastic systems with more complex microstructural arrangements and local rheologies. Some of the results can be extended to nonlinear rheologies as already indicated in the first part of this work. Other results can be exploited in studies of reinforced polymers exhibiting thermo-viscoelastic local rheologies characterized by multiple branches that are sensitive to temperature, or in studies of polycrystalline media where other incremental homogenization schemes have proved of limited use (e.g. [15]). These studies are on-going and will be reported upon completion.

Data accessibility. All data can be reproduced with the provided information.

Authors' contributions. All the authors of this work are equal contributors, having worked together throughout the entire process of research, writing and revising. All authors agree to be accountable for all aspects of the work.

Competing interests. We declare we have no competing interests.

Funding. The work was funded by a CONICET-CNRS international collaboration through grant nos PCB-II D5054 and PICS 06400. M.I.I. acknowledges additional support by the Air Force Office of Scientific Research (USA) under award no. FA9550-19-1-0377; N.L. and P.S. acknowledge additional support from Excellence Initiative of Aix-Marseille University - A*MIDEX, a French 'Investissements d'Avenir' programme in the framework of the Labex MEC.

Appendix A. Linearization procedure

The effective response of linear viscoelastic composites satisfies the superposition principle. Thus, the macroscopic stress at a given instant depends on the entire macroscopic strain history in such a way that

$$\overline{\boldsymbol{\sigma}}(t) = \mathbf{F}\,[\overline{\boldsymbol{\varepsilon}}[t]] = \mathbf{F}\,[\overline{\boldsymbol{\varepsilon}}_1[t]] + \mathbf{F}\,[\overline{\boldsymbol{\varepsilon}}_2[t]] = \overline{\boldsymbol{\sigma}}_1(t) + \overline{\boldsymbol{\sigma}}_2(t) \tag{A 1}$$

for any pair of strain histories $\overline{\boldsymbol{\varepsilon}}_1[t]$ and $\overline{\boldsymbol{\varepsilon}}_2[t]$ such that $\overline{\boldsymbol{\varepsilon}}[t] = \overline{\boldsymbol{\varepsilon}}_1[t] + \overline{\boldsymbol{\varepsilon}}_2[t]$. This superposition is also satisfied by the underlying microscopic fields of the various strain histories; thus,

$$\boldsymbol{\varepsilon}(\mathbf{x}, t) = \boldsymbol{\varepsilon}_1(\mathbf{x}, t) + \boldsymbol{\varepsilon}_2(\mathbf{x}, t) \quad \text{and} \quad \boldsymbol{\sigma}(\mathbf{x}, t) = \boldsymbol{\sigma}_1(\mathbf{x}, t) + \boldsymbol{\sigma}_2(\mathbf{x}, t). \tag{A 2}$$

The first and second moments of these fields over each phase are thus related by

$$\langle \boldsymbol{\varepsilon} \rangle^{(r)} = \langle \boldsymbol{\varepsilon}_1 \rangle^{(r)} + \langle \boldsymbol{\varepsilon}_2 \rangle^{(r)}, \quad \langle \boldsymbol{\varepsilon}^2 \rangle^{(r)} = \langle \boldsymbol{\varepsilon}_1^2 \rangle^{(r)} + \langle \boldsymbol{\varepsilon}_2^2 \rangle^{(r)} + 2\,\langle \boldsymbol{\varepsilon}_1 \cdot \boldsymbol{\varepsilon}_2 \rangle^{(r)}, \tag{A 3}$$

and similarly for the stress fields. These compositions can be carried out with an arbitrary number of independent strain histories.

By contrast, the reduced free-energy density generated by the mean-field homogenization scheme of Lahellec & Suquet [1] is non-convex and therefore the ensuing macroscopic response does not satisfy this linear superposition. However, the superposition can be imposed by applying the scheme to each strain history separately and taking the composition as a linearized estimate, that is,

$$\overline{\boldsymbol{\sigma}}(t) = \mathbf{F}_{red}\,[\overline{\boldsymbol{\varepsilon}}[t]] \approx \mathbf{F}_{red}\,[\overline{\boldsymbol{\varepsilon}}_1[t]] + \mathbf{F}_{red}\,[\overline{\boldsymbol{\varepsilon}}_2[t]]\,. \tag{A 4}$$

Given that the reduced estimates have been found to be very accurate for certain strain histories but not for others, accurate estimates for the disfavoured strain histories can be generated by decomposing them into two or more favoured strain histories and composing the corresponding stress histories following (A 4). Estimates for the first moments of the underlying strain and stress fields over each phase can also be computed by composing the corresponding moments following $(\text{A } 3)_1$. Estimates for the second moments, on the other hand, require a further approximation in view of the cross-moment in expression $(\text{A } 3)_2$. Making use of the Cauchy–Schwarz inequality as in the companion paper, this cross-moment can be bounded by

$$\langle \boldsymbol{\varepsilon}_1 \cdot \boldsymbol{\varepsilon}_2 \rangle^{(r)} \lessgtr \langle \boldsymbol{\varepsilon}_1 \rangle^{(r)} \cdot \langle \boldsymbol{\varepsilon}_2 \rangle^{(r)} \pm C_{\varepsilon_1}^{(r)^{1/2}}\, C_{\varepsilon_2}^{(r)^{1/2}}, \tag{A 5}$$

where $C_{\varepsilon_i}^{(r)}$ refers to the second moments of the intraphase fluctuations of the field $\boldsymbol{\varepsilon}_i$. The sense of the bound depends on the sign adopted on the right-hand side. In any case, the right-hand side can be used to approximate the cross-moment and generate a decomposition for the reduced second moments of the form

$$\langle \boldsymbol{\varepsilon}^2 \rangle^{(r)} \approx \langle \boldsymbol{\varepsilon}_1^2 \rangle^{(r)} + \langle \boldsymbol{\varepsilon}_2^2 \rangle^{(r)} + 2\,\langle \boldsymbol{\varepsilon}_1 \rangle^{(r)} \cdot \langle \boldsymbol{\varepsilon}_2 \rangle^{(r)} \pm 2\, C_{\varepsilon_1}^{(r)^{1/2}}\, C_{\varepsilon_2}^{(r)^{1/2}}, \tag{A 6}$$

and similarly for the second moments of the stress field. Of course, analogous identities can be written for the mean and deviatoric parts or any other set of orthogonal projections of fields taken independently, as in (2.4).

In the particular case of rigidly reinforced solids considered in this study, the approximation (A 5) can be dispensed with by exploiting Hill's lemma. Indeed, this lemma implies that

$$\overline{\boldsymbol{\varepsilon}}_1 \cdot \overline{\boldsymbol{\sigma}}_2 = \langle \boldsymbol{\varepsilon}_1 \cdot \boldsymbol{\sigma}_2 \rangle = (1-c)\left(9\kappa\,\langle \varepsilon_{1_m} \varepsilon_{2_m} \rangle^{(1)} + 2\mu_{0_2}\,\langle \boldsymbol{\varepsilon}_{1_d} \cdot \boldsymbol{\varepsilon}_{2_d} \rangle^{(1)} + \boldsymbol{\tau}_{0_2} \cdot \langle \boldsymbol{\varepsilon}_{1_d} \rangle^{(1)}\right), \tag{A 7}$$

where μ_{0_2} and $\boldsymbol{\tau}_{0_2}$ are the comparison modulus and stress polarization, respectively, associated with the reduced estimates for the strain history $\overline{\boldsymbol{\varepsilon}}_2[t]$. By the same token,

$$\overline{\boldsymbol{\varepsilon}}_2 \cdot \overline{\boldsymbol{\sigma}}_1 = \langle \boldsymbol{\varepsilon}_2 \cdot \boldsymbol{\sigma}_1 \rangle = (1-c)\left(9\kappa\,\langle \varepsilon_{1_m} \varepsilon_{2_m} \rangle^{(1)} + 2\mu_{0_1}\,\langle \boldsymbol{\varepsilon}_{1_d} \cdot \boldsymbol{\varepsilon}_{2_d} \rangle^{(1)} + \boldsymbol{\tau}_{0_1} \cdot \langle \boldsymbol{\varepsilon}_{2_d} \rangle^{(1)}\right). \tag{A 8}$$

These two equations can be used to compute the cross-moments $\langle \boldsymbol{\varepsilon}_{1_d} \cdot \boldsymbol{\varepsilon}_{2_d} \rangle^{(1)}$ and $\langle \varepsilon_{1_m} \varepsilon_{2_m} \rangle^{(1)}$ in terms of the known macroscopic strains and stresses exactly. Now, these exact relations can be used to assess the accuracy of the approximation (A 6) being proposed for more general material systems.

We conclude this exposition by noting that the results reported in §§3 and 4 suggest Heaviside steps may constitute strain histories of particular relevance for this linearization procedure. Indeed, those results suggest that the reduced estimates are particularly problematic when the norm of the macroscopic strain tends to vanish. In such cases, a possible remedy is to decompose the strain history as $\overline{\boldsymbol{\varepsilon}}(t) = [\overline{\boldsymbol{\varepsilon}}(t) + H(t)\,\overline{\boldsymbol{\varepsilon}}'] + [-H(t)\,\overline{\boldsymbol{\varepsilon}}']$, where $H(t)$ denotes the Heaviside function and $\overline{\boldsymbol{\varepsilon}}'$ is a constant strain such that the norm $||\overline{\boldsymbol{\varepsilon}}(t) + H(t)\,\overline{\boldsymbol{\varepsilon}}'||$ is sufficiently large for the entire history. Interestingly, the contribution of the second term to the stresses decays exponentially with a certain characteristic time. After a few such characteristic times, the stresses are thus entirely due to the first strain history, and hence do not require additional computational effort.

References

1. Lahellec N, Suquet P. 2007 Effective behavior of linear viscoelastic composites: a time-integration approach. *Int. J. Solids Struct.* **44**, 507–529. (doi:10.1016/j.ijsolstr.2006.04.038)
2. Idiart MI, Lahellec N, Suquet P. 2020 Model reduction by mean-field homogenization in viscoelastic composites. I. Primal theory. *Proc. R. Soc. A* 20200407. (doi:10.1098/rspa.2020.0407)
3. Dvorak G. 1992 Transformation field analysis of inelastic composite materials. *Proc. R. Soc. Lond. A* **437**, 311–327. (doi:10.1098/rspa.1992.0063)
4. Michel JC, Suquet P. 2003 Nonuniform transformation field analysis. *Int. J. Solids Struct.* **40**, 6937–6955. (doi:10.1016/S0020-7683(03)00346-9)
5. Suquet P. 2012 Four exact relations for the effective relaxation function of linear viscoelastic composites. *C. R. Mecanique* **340**, 387–399. (doi:10.1016/j.crme.2012.02.022)
6. Idiart MI, Lahellec N. 2016 Estimates for the overall linear properties of pointwise heterogeneous solids and application to elasto-viscoplasticity. *J. Mech. Phys. Solids* **97**, 317–332. (doi:10.1016/j.jmps.2015.12.017)
7. Willis JR. 1982 Elasticity theory of composites. In *Mechanics of solids* (eds HG Hopkins, MJ Sewell), The Rodney Hill 60th Anniversary Volume, pp. 653–686. Oxford, UK: Pergamon Press.
8. Ricaud J-M, Masson R. 2009 Effective properties of linear viscoelastic heterogeneous media: internal variables formulation and extension to ageing behaviours. *Int. J. Solids Struct.* **46**, 1599–1606. (doi:10.1016/j.ijsolstr.2008.12.007)
9. Mandel J. 1966 *Cours de mécanique des milieux continus*. Paris, France: Gauthier-Villars.
10. Boudet J, Auslender F, Bornert M, Lapusta Y. 2016 An incremental variational formulation for the prediction of the effective work-hardening behaviour and field statistics of elasto-(visco)plastic composites. *Int. J. Solids Struct.* **83**, 90–113. (doi:10.1016/j.ijsolstr.2016.01.003)
11. Lucchetta A, Auslender F, Bornert M, Kondo D. 2019 A double incremental variational procedure for elastoplastic composites with combined isotropic and linear kinematic hardening. *Int. J. Solids Struct.* **158**, 243–267. (doi:10.1016/j.ijsolstr.2018.09.012)
12. Lahellec N, Suquet P. 2007 On the effective behavior of nonlinear inelastic composites: I. Incremental variational principles. *J. Mech. Phys. Solids* **55**, 1932–1963. (doi:10.1016/j.jmps.2007.02.003)
13. Beurthey S, Zaoui A. 2000 Structural morphology and relaxation spectra of viscoelastic heterogeneous materials. *Eur. J. Mech. A Solids* **19**, 1–16. (doi:10.1016/S0997-7538(00)00157-1)
14. Laws N, McLaughlin R. 1978 Self-consistent estimates for the viscoelastic creep compliance of composite materials. *Proc. R. Soc. Lond. A* **359**, 251–273. (doi:10.1098/rspa.1978.0041)
15. Badulescu C, Lahellec N, Suquet P. 2015 Field statistics in linear viscoelastic composites and polycrystals. *Eur. J. Mech. A Solids* **49**, 329–344. (doi:10.1016/j.euromechsol.2014.07.012)